Ligand and membrane-binding behavior of the phosphatidylinositol transfer proteins PITPα and β

Matilda Baptist[1], Candace Panagabko[1], Shamshad Cockcroft[2], Jeffrey Atkinson[1*]

[1] Department of Chemistry and Centre for Biotechnology, Brock University, St. Catharines, Ontario, L2A 3S1, Canada

[2] Department of Neuroscience, Physiology and Pharmacology, University College London, London WC1E 6JJ, UK.

[*] Corresponding Author: Jeffrey Atkinson (e-mail: jatkinson@brocku.ca)

Abstract

Phosphatidylinositol transfer proteins (PITPs) are believed to be lipid transfer proteins due to their ability to transfer either PI or PC between membrane compartments *in vitro*. However, the detailed mechanism of this transfer process is not fully established. To further understand the transfer mechanism of PITPs we examined the interaction of PITPs with membranes using dual polarization interferometry (DPI) which measures protein binding affinity on a flat immobilized lipid surface. In addition, a fluorescence resonance energy transfer (FRET)-based assay was also employed to monitor how quickly PITPs transfer their ligands to lipid vesicles. DPI analysis revealed that PITPβ had a higher affinity to membranes compared to PITPα. Furthermore, the FRET-based transfer assay revealed that PITPβ has a higher ligand transfer rate compared to PITPα. However, both PITPα and PITPβ demonstrated a preference for highly curved membrane surfaces during ligand transfer. In other words, ligand transfer rate was higher when the accepting vesicles were highly curved.

Keywords phosphatidylinositol transfer protein · dual polarization interferometry · fluorescence resonance energy transfer, protein-membrane binding

Introduction

Class I phosphatidylinositol transfer proteins (PITPs) in humans consist of both PITPα and PITPβ that share 77% sequence identity and 94% sequence similarity (Carvou et al. 2010). PITPs are small soluble proteins with a molecular weight of ~32 kDa. They possess a lipid-binding cavity that accommodates a single phospholipid molecule (Cockcroft and Carvou 2007). The lipid-binding cavity is made up of eight β-strands and two α-helices. The hydrophobic pocket is closed by a 'lid' region made up of the C-terminal portion and an 11 amino acid extension (Vordtriede et al. 2005; Yoder et al. 2001). A superimposition of rat PITPα and β structures is shown in **Figure 1**. PITPα and PITPβ possess dual specificity for both phosphatidylcholine (PC) and phosphatidylinositol (PI) with a 16-fold higher affinity for PI (de Brouwer et al. 2002). PITPs have been portrayed as lipid transfer proteins due to their ability to transfer PI or PC between membrane compartments *in vitro*.

To date, through structural analyses, we understand that PITPs adopt an open and closed conformation. The open conformation occurs only when PITP is docked to membranes with the 'lid' being displaced exposing hydrophobic residues (Schouten et al. 2002; Tilley et al. 2004). This 'lid' displacement is thought to allow PITPs to pick up or deposit its ligand from or into membranes. Two tryptophan residues, namely W203 and W204, have been identified to play a role in PITP's docking to membranes. W203 and W204 are located on the loop between β-strand 8 (residues 191-201) and α-helix F (residues 206-236) (Tilley et al. 2004). The x-ray structure shows that both tryptophan residues are exposed as opposed to being buried within the protein core. Mutation of both tryptophan residues to alanine resulted in a loss of PITP membrane binding and consequently lipid transfer (Shadan et al. 2008; Tilley et al. 2004; Yadav et al. 2015). From these observations, it was proposed that PITPs transfer ligand in the closed conformation, protecting their hydrophobic ligand from the surrounding aqueous environment. However, upon docking to membranes, PITPs adopt an open conformation to undergo ligand exchange. The Orientation of Proteins in Membranes database (Lomize et al. 2012) provides a calculated orientation of both PITPs with respect to a model hydrophobic membrane – **Figure 2**. The approaches of the two proteins are similar, but not identical, with PITPβ penetrating deeper into the membrane (4.7 ± 1.7 Å) than PITPα (2.3 ± 1.9 Å). However, both proteins have similar free energies of transfer; $\Delta G_{transfer}$ = -4.1 kcal/mol for PITPα and -4.3 kcal/mol for PITPβ□

The detailed ligand transfer mechanism of PITPs remains to be fully established. Here, we investigated the membrane association of PITPα and PITPβ in order to gain a better understanding of the ligand transfer mechanism of PITPs. Using DPI we examined PITP binding affinity to a planar immobilized lipid layer. In addition, we measured the rate at which PITPα and PITPβ transfer NBD-PC to lipid vesicles using a FRET-based transfer assay. DPI analysis revealed a higher membrane affinity for PITPβ compared to PITPα, which was reflected in a higher ligand transfer rate for PITPβ compared to PITPα. Furthermore, FRET experiments established that both PITPs prefer highly curved membrane surfaces during ligand transfer.

Materials and Methods

Protein Expression and Purification

PITPα and PITPβ were expressed from pRSET vectors (Shadan et al. 2008). PITPα mutants were generated using the Quikchange protocol using *PfuTurbo* DNA polymerase (Agilent Technologies, Santa Clara, USA). The pRSET construct of human PITPα served as the template to create the following mutants: W203A/W204A, C95A and K61A. All primers utilized were designed using either PrimerX or OligoPerfect Designer and were manufactured by Sigma-Aldrich (Oakville, Canada). The desired mutations were confirmed by DNA sequencing at Robarts Research Institute (London, Canada). All His-tagged PITP proteins were expressed in the *E. coli* BL21(DE3)pLysS cells (Sigma, Oakville, Canada). *E. coli* cultures were grown at 37 °C until an OD_{600} of 0.4 to 0.6 was obtained. Subsequently the cultures were induced with 0.4 mM IPTG (Bioshop, Burlington, Canada) overnight at 28 °C except for C95A which was at 20 °C. The cells were harvested by centrifugation and stored at -80 °C until further use.

Cell pellets were re-suspended in re-suspension buffer (50 mM KH_2PO_4, 300 mM NaCl, 10 % glycerol, pH 7.5). 0.5 % Triton-X and DNase I (2 units/mL lysate) was added to the cell suspension followed by one tablet of ProteoGuard EDTA-free protease inhibitor (Clontech, Mountain View, USA). The cell suspension was allowed to incubate on ice for 15 min. The cell supernatant was obtained by centrifugation at 13682 *g* for 40 min at 4 °C and added to a column containing 1 mL TALON metal affinity resin (Clontech, Mountain View, USA). Subsequently the resin was washed with 10 mL re-suspension buffer containing 20 mM imidazole. Protein was eluted with 5 mL elution buffer (50 mM KH_2PO_4, 300 mM NaCl, 150 mM imidazole, 10 % glycerol, pH 7.5). Finally the protein was exchanged into PIPES buffer (20 mM PIPES, 137 NaCl, 2.7 mM KCl, pH 6.8). The resin was regenerated with resin regeneration buffer (20 mM MES (2-(N-morpholino)ethanesulfonic acid), 100 mM NaCl, pH 5). Purified protein was subject

to SDS-PAGE analysis and quantified using Bradford assay. Pure PITP proteins were stored at 4 °C and typically used within 5 days of purification.

Fluorescence-based Binding Assay

All PITP proteins were subject to a fluorescence-based binding assay using NBD-PC (Life Technologies, Burlington, Canada), a fluorescent analog of PC. Briefly, a final protein concentration of 0.2 μM in TKE buffer (50 mM Tris, 100 mM KCl, 1 mM EDTA, pH 7.4) was titrated with increasing NBD-PC concentrations from ethanol stock solutions. The fluorescence spectrum was measured between 515 and 550 nm while the excitation wavelength was set at 469 nm. The fluorescence at 527 nm was applied to the following equation provided by GraphPad Prism (GraphPad Software, La Jolla, USA) to obtain the equilibrium dissociation constant, K_d:

$$Y = B_{max}.X / K_d + X \qquad (1)$$

Y represents specific binding, B_{max} is the maximum number of binding sites and X is the ligand concentration.

Reduction of NBD-PC by Sodium Hydrosulfite

The reduction of NBD-PC bound to PITP was performed by incubating 2 μM protein in TKE buffer with 0.2 μM NBD-PC for 15 min at room temperature on a rotator. The protein-ligand mixture was then titrated with 4 mM sodium hydrosulfite and the change in fluorescence was observed at 532 nm over time. The excitation wavelength was set at 469 nm. A rate constant for fluorophore reduction was obtained using a one-phase exponential decay equation provided by GraphPad Prism:

$$Y = Span.e^{-k.X} + Plateau \qquad (2)$$

Y represents fluorescence intensity, X is time and k is the rate constant.

Lipid Vesicle Preparation

Both large and small unilamellar vesicles (LUVs/SUVs) were prepared as described previously (Zhang et al. 2009). Vesicles used for DPI analysis were prepared in DPI running buffer (10mM K_2HPO_4, 137 mM NaCl, pH 7.4) while vesicles for the FRET-based transfer assays were prepared in TKE buffer. The mean diameter of vesicles was determined by dynamic light scattering using Protein Solutions DynaPro-99-E (Wyatt Technologies, Santa Barbara, USA). The average diameters of LUVs prepared by extrusion through 100 nm polycarbonate filters were 150 nm with a polydispersity index of 0.15 while SUVs prepared by probe sonication were 29 nm with a polydispersity index of 0.12.

Dual Polarization Interferometry Analysis of PITP Binding to Membranes

DPI analysis was performed using the Analight Bio200 (Biolin Scientific, New Jersey, USA). The procedure and data manipulation used here were similar to those described previously (Baptist et al. 2015) with minor changes. 800 µL of lipid and protein samples were used for each injection. Regeneration of the sensor chip was achieved using 2 % SDS solution followed by 80 % EtOH.

FRET-based Transfer Assay

The transfer of NBD-PC by PITPs to lipid vesicles was examined using a FRET-based assay as described previously (Zhang et al. 2009). All experiments were conducted using a QuantaMaster-QM-2001-4 spectrofluorometer (Horiba Scientific, London, Canada). Briefly, 4 µM protein was incubated with 0.4 µM NBD-PC for 15 min on a rotator in TKE buffer. The protein-ligand mixture was mixed with 200 µM acceptor vesicles containing 3 mol% lissamine rhodamine B (fluorescence acceptor for NBD-PC) using a stopped-flow device. NBD-PC fluorescence decay was measured over time at 532 nm while the excitation wavelength was set at 469 nm. The ligand transfer rate was obtained from a two-phase exponential decay equation provided by GraphPad Prism:

$$Y=\text{Span1}.e^{-k_1.X} + \text{Span2}.e^{-k_2.X} + \text{Plateau} \qquad (3)$$

where Y represents the normalized fluorescence intensity, X is time, and k_1 and k_2 are the rate constants. Only the fast rate is considered here as it corresponds to the ligand transfer rate by PITP. The slow rate is 20-30 times slower and is likely due to a small proportion of photobleaching of the NBD-PC.

Results & Discussion

Affinity of PITPs to NBD-PC

Prior to performing the FRET-based transfer assay, the affinity of PITPs to NBD-PC was determined using a fluorescence-based binding assay. All the proteins tested showed the capacity to bind NBD-PC with a K_d < ~150 nM which is characteristic of high affinity binding in most biological systems – **Table 1**.

Reduction of NBD-PC bound to PITPs

From our binding assay data it was interesting to note that both C95A and BSA demonstrated a high affinity for NBD-PC. C95A has been previously shown to lack the capacity to transfer PC (Carvou et al. 2010). BSA on the other hand was used as a control protein as it functions as a lipid-binding protein but lacks the PITP ligand binding pocket (Huang et al. 2004). However, it was observed that the maximum fluorescence for both C95A and BSA was substantially lower than that of wild-type PITPα. Therefore, we conducted an NBD-PC reduction assay to explore the nature of the binding variation of NBD-PC by PITPs namely PITPα, PITPβ and C95A. Our data revealed that C95A bound NBD-PC was reduced 4 to 5-times faster compared to PITPα and PITPβ – **Table 2**. This result was anticipated since C95A exhibited a low maximum fluorescence in the binding assay. The NBD group is sensitive to its

environment in that it fluoresces more prominently in a hydrophobic environment as opposed to polar surroundings (Chattopadhyay 1990). The lower fluorescence reading when using C95A indicates that NBD-PC is bound in such a way that the NBD portion is more solvent exposed. The faster NBD reduction rate further confirms this notion. The NBD-PC group may also equilibrate more quickly from the protein (*i.e.* a fast k_{off}) and is thus more accessible for reduction by sodium hydrosulfite.

DPI analysis of PITP binding to membranes

The affinity of PITPα and PITPβ to DOPC lipid layers was determined by DPI analysis. Both PITPα and PITPβ bound to DOPC lipid layers with K_d of 1.85 ± 0.47 μM and 0.81 ± 0.45 μM respectively – **Figure 3**. The maximum specific bound mass of protein (B_{max} values) obtained for both PITPα and PITPβ are as follows: 0.53 ± 0.06 ng/mm^2 and 0.42 ± 0.09 ng/mm^2. Despite having similar B_{max} values, and appreciating that these measurements are only duplicates, the K_d of PITPβ appears to be nearly two-fold lower compared to PITPα. This implies that PITPβ has a higher affinity for DOPC lipid layers than PITPα. An attempt was made to measure the binding of the PITPα mutant, W203A/W204A, to DOPC lipid layers, however, no binding was observed. This result was expected since the W203A/W204A mutant lacks the capability to bind and transfer ligand to membranes (Shadan et al. 2008; Yadav et al. 2015).

We also wondered whether a measured protein affinity for a membrane bilayer might depend on the protein carrying a phospholipid molecule. Thus, we measured membrane affinity of PITPα and PITPβ at 0.5 μM protein concentration that had been pre-incubated with either PC or PI and the amount of ligand-bound PITPs that bound to DOPC lipid layers were determined using DPI. There was no difference (unpaired t-test, p = 0.8058) in the amount of PITPα bound to DOPC lipid layers in the presence or absence of PC – **Figure 4**. However, ~70% less PITPα bound to DOPC lipid layers when the protein was pre-incubated with PI (p = 0.0099). PITPβ bound to a membrane bilayer about half as well when pre-incubated with PC but the data was not statistically significant (p = 0.3583). Interestingly, no binding mass data could be extracted for PITPβ when the protein was pre-incubated with PI. Our investigation reveals that PI-bound PITPs have much lower affinity for membranes. PITP clearly gives up its ligand during the FRET based transfer assays, as it delivers NBD-PC to acceptor vesicles. However, when the

protein is first allowed to bind PI (for which it has a significantly higher affinity than PC) it appears unable to form an adsorbed protein layer on the immobilized membrane. Our lack of a fluorescent PI analogue made this impossible to test using FRET-based transfer assays. The failure of PITPβ with bound PI to adsorb to a membrane would certainly suggest that it would be, at best, a poor catalyst for the transfer of PI to membranes. Early in vitro PI transfer assays using bovine brain PITP (Somerharju and Wirtz 1982; Zborowski and Demel 1982a, b) may represent only basal, background ability that is only apparent in assays where this is the only activity being observed. This would seem to be counter to what a true transfer protein should do. Indeed, several "transfer" proteins are now being re-evaluated for their real role in vivo. For example, the role of the prototypical phospholipid transfer protein from yeast, Sec14, was thought to be a PI transfer protein for many years, but is now being re-evaluated in terms of a mechanism of PI presentation to PI-kinases (Bankaitis et al. 2007; Mousley et al. 2006; Schaaf et al. 2008). In such a case, Sec14 must have an affinity for membrane resident PI, but it only assists in the partial extraction of PI from the membrane so that PI-kinases have access to their substrate. Indeed, PITPs have been linked to the production of phosphoinositides. Two models have been proposed to describe the role of PITPs in this process: the PI delivery model and the PI presentation model (Cockcroft 2012). The PI delivery model simply proposes that the sole function of PITP is to deliver PI from the ER to other non-ER membranes for the generation of phosphoinositides. In contrast, the PI presentation model suggests that PITP functions to present its ligand to lipid kinases for the production of phosphoinositides (Bankaitis et al. 2012). While ours are in vitro experiments, it would seem dysfunctional for a true transfer protein to lose affinity for a membrane when bound to its favored ligand PI. This would compromise the ability to deliver the PI to a receiving membrane. The fact that following pre-incubation with PI both PITPα and PITPβ show less bound mass to immobilized bilayers (**Figure 4**) supports this claim. In these cases, the PITP may be extracting the PI from the membrane, lowering the protein-membrane affinity and thus desorbing from the surface. In other words, PI-bound PITP may be trying to present PI to lipid kinases (possibly through protein-protein interactions) but, finding none, extracts the ligand and leaves the membrane surface. This suggestion is still preliminary, however, and requires further investigation.

Ligand transfer rates of PITPs determined by FRET

Using a FRET-based assay and the fluorescent analog of PC (NBD-PC), the ligand transfer rates were measured for the movement of PITP-bound NBD-PC to PC vesicles. Prior to obtaining the ligand transfer rates of PITPs, a series of control studies were performed. In the absence of both protein and lipid vesicles, it was observed that NBD-PC demonstrated negligible background fluorescence – **Figure 5**. This is consistent with the characteristics of NBD whereby it fluoresces weakly in polar versus hydrophobic environments (Chattopadhyay 1990). The rate of spontaneous transfer of NBD-PC to lipid vesicles was also determined. Lipid vesicles were prepared that did not contain FRET acceptor. In this case the fluorescence should increase as the free NBD-PC diffuses into the more hydrophobic vesicle membrane. The rate of spontaneous transfer of NBD-PC to lipid vesicles was determined to be negligible over the time frame of our transfer assays – **Figure 5**. The fluorescence count when NBD-PC was incorporated into lipid vesicles at 0.2 mol% was determined to be within 250000 – 270000 (data not shown). Thus, if all the NBD-PC used in this assay successfully transferred to lipid vesicles, the fluorescence count should rise to this level, but it did not. Thus, over the course of our transfer assays there is a negligible rate of spontaneous transfer of NBD-PC to lipid vesicles. This means that in experiment with PITPs, any NBD-PC fluorescence quenching observed due to its arrival at the vesicle bilayer is solely the result of protein-catalyzed transfer and not to spontaneous transfer.

In addition, little fluorescence signal decay was observed when NBD-PC bound to protein was monitored in the absence of lipid vesicles – **Figure 6**. This observation reveals three things: 1) loss of fluorescence from NBD-PC bound to protein was only observed when lipid vesicles were present; 2) the concentration used for both protein and NBD-PC was sufficient to produce an observable fluorescence count; 3) <5% of photo-bleaching of the NBD-PC fluorescence signal was observed within the time frame of measurement. Thus our FRET-based transfer assay proved to be a reliable technique in measuring protein ligand transfer to lipid vesicles.

The FRET-based assay revealed that both PITPα and PITPβ have the capacity to transfer NBD-PC to lipid vesicles. Both PITPs have a higher ligand transfer rate to SUVs than to LUVs – **Figure 7**. In fact, no transfer was observed for PITPα with LUVs. In other words PITPs show a preference for highly curved membrane surfaces during ligand transfer. This difference in rate is not due to an increase in lipid area during the preparation of SUVs versus LUVs. We have considered this previously (Zhang et al. 2009) where we calculated that the area available on the

outer leaflet of vesicles increases by only 1.5 times when vesicle size is reduced from 200 nm to 20 nm when an equal amount of phospholipid is used.

Interestingly, PITPβ transferred NBD-PC to vesicles nearly twice as fast as PITPα. It should be noted that the lipid concentration used for each protein was different only because the ligand transfer rate for PITPβ was too fast for easy capture by our stopped flow setup. Consequently, the concentration of lipid vesicles was reduced by half - from a final concentration (after mixing of lipids and protein solution) of 100 μM to 50 μM for PITPβ transfer measurements. Thus, in our *in vitro* assay, PITPβ is able to transfer NBD-PC to phospholipid bilayers as much as four times faster than PITPα.

The ligand transfer rates of the PITPα mutants were also determined. Our data confirmed that both W203A/W204A and C95A mutants are unable to transfer NBD-PC to lipid vesicles – **Figure 8**. These observations were anticipated since W203A/W204A mutant lacks the ability to bind to membranes while C95A is thought to be a poor binder of PC. Despite the high affinity of C95A to NBD-PC from our fluorescence binding assay, our NBD-PC reduction and FRET assay supports that C95A is a poor binder of PC. The high affinity observed for C95A toward NBD-PC may imply that the ligand is still bound to the protein but in a different manner than wild type PITPα. Even though the ligand is still bound to C95A, it is bound in a way that the protein is unable to deliver the ligand to membranes. The PITPα K61A mutant, which lacks the ability to bind PI but is still able to bind to PC, showed approximately the same transfer rate for NBD-PC as wild type PITPα – **Figure 7**.

Conclusion

Our results not only demonstrate the ability of PITPs to bind to membranes but also to transfer its natural PC-ligand analogue NBD-PC to lipid vesicles. Interestingly, DPI analysis showed that PITPβ possessed a nearly two-fold higher affinity for membranes compared to PITPα. In addition, our FRET-based assay showed that PITPβ has a faster ligand transfer rate than PITPα again by two to four-fold. Data obtained from this study supports the results of Shadan *et al.* (Shadan et al. 2008). These authors investigated membrane interactions of both PITPα and PITPβ in intact cells using N-ethylmaleimde to trap the protein at the membrane.

PITPβ appeared to have a higher affinity for membranes than PITPα (Shadan et al. 2008). Within the ten-minute time frame of their assays, almost all of PITPβ were found to be membrane-associated compared to only about 50% of PITPα. The reasons behind this difference remain to be established in detail, but might include the slightly favored calculated $\Delta G_{transfer}$ to membranes for PITPβ of -4.3 kcal/mol over that of PITPα □□□–4.1□□□□□□□□□□ (Lomize et al. 2013).

Our studies also reveal that PITPs prefer to bind to highly curved membrane surfaces. In recent years, several lipid transfer proteins have been shown to have a propensity for highly curved membrane surfaces (Lev 2010). Some lipid transfer proteins, such as the ceramide transfer protein (CERT) (Tuuf et al. 2011) have shown a preference for more fluid membrane environments, which suggests that transfer proteins can be sensitive to lipid order in membranes. Highly curved membrane surfaces or loosely packed membrane environments provide easier access for proteins to insert hydrophobic residues past the head group region into the central core of the membrane (Lomize and Pogozheva 2013; Lomize et al. 2007; Pogozheva et al. 2014; Pogozheva et al. 2013). Therefore it is not surprising for the PITPs to show a similar preference, especially considering the critical importance of W203 and W204 to membrane binding (Tilley et al. 2004; Yau et al. 1998). Studies are revealing that one of the major ways peripheral proteins are recruited to membranes is through the recognition of physicochemical parameters of membranes which include curvature and lipid packing (Bigay and Antonny 2012). Our results support that PITPs may be recruited to membranes via this mechanism.

References

Bankaitis, V.A., Ile, K.E., Nile, A.H., Ren, J., Ghosh, R., and Schaaf, G. 2012. Thoughts on Sec14-like nanoreactors and phosphoinositide signaling. Adv Biol Regul **52**(1): 115-121. doi: 10.1016/j.jbior.2011.11.001. PMID: 22776890

Bankaitis, V.A., Vincent, P., Merkulova, M., Tyeryar, K., and Liu, Y. 2007. Phosphatidylinositol transfer proteins and functional specification of lipid signaling pools. Adv Enzyme Regul **47**: 27-40. PMID: 17335879

Baptist, M., Panagabko, C., Nickels, J.D., Katsaras, J., and Atkinson, J. 2015. 2,2'-Bis(monoacylglycero) PO4 (BMP), but Not 3,1'-BMP, increases membrane curvature stress to enhance alpha-tocopherol transfer protein binding to membranes. Lipids **50**(3): 323-328. doi: 10.1007/s11745-015-3989-9. PMID: 25603781

Bigay, J., and Antonny, B. 2012. Curvature, lipid packing, and electrostatics of membrane organelles: defining cellular territories in determining specificity. Dev Cell **23**(5): 886-895. doi: 10.1016/j.devcel.2012.10.009. PMID: 23153485

Carvou, N., Holic, R., Li, M., Futter, C., Skippen, A., and Cockcroft, S. 2010. Phosphatidylinositol- and phosphatidylcholine-transfer activity of PITPbeta is essential for COPI-mediated retrograde transport from the Golgi to the endoplasmic reticulum. J Cell Sci **123**(Pt 8): 1262-1273. doi: 10.1242/jcs.061986. PMID: 20332109

Chattopadhyay, A. 1990. Chemistry and biology of N-(7-nitrobenz-2-oxa-1,3-diazol-4-yl)-labeled lipids: fluorescent probes of biological and model membranes. Chem Phys Lipids **53**(1): 1-15. PMID: 2191793

Cockcroft, S. 2012. The diverse functions of phosphatidylinositol transfer proteins. Curr Top Microbiol Immunol **362**: 185-208. doi: 10.1007/978-94-007-5025-8_9. PMID: 23086419

Cockcroft, S., and Carvou, N. 2007. Biochemical and biological functions of class I phosphatidylinositol transfer proteins. Biochim Biophys Acta **1771**(6): 677-691. doi: 10.1016/j.bbalip.2007.03.009. PMID: 17490911

de Brouwer, A.P., Versluis, C., Westerman, J., Roelofsen, B., Heck, A.J., and Wirtz, K.W. 2002. Determination of the stability of the noncovalent phospholipid transfer protein-lipid complex by electrospray time-of-flight mass spectrometry. Biochemistry **41**(25): 8013-8018. PMID: 12069592

Huang, B.X., Kim, H.Y., and Dass, C. 2004. Probing three-dimensional structure of bovine serum albumin by chemical cross-linking and mass spectrometry. J Am Soc Mass Spectrom **15**(8): 1237-1247. doi: 10.1016/j.jasms.2004.05.004. PMID: 15276171

Lev, S. 2010. Non-vesicular lipid transport by lipid-transfer proteins and beyond. Nat Rev Mol Cell Biol **11**(10): 739-750. doi: nrm2971 [pii]

10.1038/nrm2971 [doi]. PMID: 20823909

Lomize, A., Lomize, M., and Pogozheva, I. 2013. Orientaions of proteins in membranes. Available from http://opm.phar.umich.edu/protein.php?search=2a1l2016%5D.

Lomize, A.L., and Pogozheva, I.D. 2013. Solvation models and computational prediction of orientations of peptides and proteins in membranes. Methods Mol Biol **1063**: 125-142. doi: 10.1007/978-1-62703-583-5_7. PMID: 23975775

Lomize, A.L., Pogozheva, I.D., Lomize, M.A., and Mosberg, H.I. 2007. The role of hydrophobic interactions in positioning of peripheral proteins in membranes. BMC Struct Biol **7**: 44. PMID: 17603894

Lomize, M.A., Pogozheva, I.D., Joo, H., Mosberg, H.I., and Lomize, A.L. 2012. OPM database and PPM web server: resources for positioning of proteins in membranes. Nucleic Acids Res **40**(Database issue): D370-376. doi: 10.1093/nar/gkr703. PMID: 21890895

Mousley, C.J., Tyeryar, K.R., Ryan, M.M., and Bankaitis, V.A. 2006. Sec14p-like proteins regulate phosphoinositide homoeostasis and intracellular protein and lipid trafficking in yeast. Biochem Soc Trans **34**(Pt 3): 346-350. PMID: 16709158

Pogozheva, I.D., Mosberg, H.I., and Lomize, A.L. 2014. Life at the border: adaptation of proteins to anisotropic membrane environment. Protein Sci **23**(9): 1165-1196. doi: 10.1002/pro.2508. PMID: 24947665

Pogozheva, I.D., Tristram-Nagle, S., Mosberg, H.I., and Lomize, A.L. 2013. Structural adaptations of proteins to different biological membranes. Biochim Biophys Acta **1828**(11): 2592-2608. doi: 10.1016/j.bbamem.2013.06.023. PMID: 23811361

Schaaf, G., Ortlund, E.A., Tyeryar, K.R., Mousley, C.J., Ile, K.E., Garrett, T.A., Ren, J., Woolls, M.J., Raetz, C.R., Redinbo, M.R., and Bankaitis, V.A. 2008. Functional anatomy of phospholipid binding and regulation of phosphoinositide homeostasis by proteins of the sec14 superfamily. Mol Cell **29**(2): 191-206. doi: S1097-2765(07)00821-0 [pii]

10.1016/j.molcel.2007.11.026. PMID: 18243114

Schouten, A., Agianian, B., Westerman, J., Kroon, J., Wirtz, K.W., and Gros, P. 2002. Structure of apo-phosphatidylinositol transfer protein alpha provides insight into membrane association. EMBO J **21**(9): 2117-2121. doi: 10.1093/emboj/21.9.2117. PMID: 11980708

Shadan, S., Holic, R., Carvou, N., Ee, P., Li, M., Murray-Rust, J., and Cockcroft, S. 2008. Dynamics of lipid transfer by phosphatidylinositol transfer proteins in cells. Traffic **9**(10): 1743-1756. doi: 10.1111/j.1600-0854.2008.00794.x. PMID: 18636990

Somerharju, P., and Wirtz, K.W.A. 1982. Semisynthesis and Properties of a Fluorescent Phosphatidyl Inositol Analog Containing a Cis-Parinaroyl Moiety. Chemistry and Physics of Lipids **30**(1): 81-91. doi: Doi 10.1016/0009-3084(82)90009-3. PMID: WOS:A1982NM06900008

Tilley, S.J., Skippen, A., Murray-Rust, J., Swigart, P.M., Stewart, A., Morgan, C.P., Cockcroft, S., and McDonald, N.Q. 2004. Structure-function analysis of human phosphatidylinositol transfer protein alpha bound to phosphatidylinositol. Structure **12**(2): 317-326. doi: 10.1016/j.str.2004.01.013. PMID: 14962392

Tuuf, J., Kjellberg, M.A., Molotkovslcy, J.G., Hanada, K., and Mattjus, P. 2011. The intermembrane ceramide transport catalyzed by CERT is sensitive to the lipid environment. Biochimica Et Biophysica Acta-Biomembranes **1808**(1): 229-235. doi: 10.1016/j.bbamem.2010.09.011. PMID: WOS:000285853800024

Vordtriede, P.B., Doan, C.N., Tremblay, J.M., Helmkamp, G.M., Jr., and Yoder, M.D. 2005. Structure of PITPbeta in complex with phosphatidylcholine: comparison of structure and lipid transfer to other PITP isoforms. Biochemistry **44**(45): 14760-14771. PMID: 16274224

Yadav, S., Garner, K., Georgiev, P., Li, M., Gomez-Espinosa, E., Panda, A., Mathre, S., Okkenhaug, H., Cockcroft, S., and Raghu, P. 2015. RDGBalpha, a PtdIns-PtdOH transfer protein, regulates G-protein-coupled PtdIns(4,5)P2 signalling during Drosophila phototransduction. J Cell Sci **128**(17): 3330-3344. doi: 10.1242/jcs.173476. PMID: 26203165

Yau, W.M., Wimley, W.C., Gawrisch, K., and White, S.H. 1998. The preference of tryptophan for membrane interfaces. Biochemistry **37**(42): 14713-14718. doi: 10.1021/bi980809c. PMID: 9778346

Yoder, M.D., Thomas, L.M., Tremblay, J.M., Oliver, R.L., Yarbrough, L.R., and Helmkamp, G.M., Jr. 2001. Structure of a multifunctional protein. Mammalian phosphatidylinositol transfer protein complexed with phosphatidylcholine. J Biol Chem **276**(12): 9246-9252. PMID: 11104777

Zborowski, J., and Demel, R.A. 1982a. Transfer Properties of the Bovine Brain Phospholipid Transfer Protein - Effect of Charged Phospholipids and of Phosphatidylcholine Fatty-Acid Composition. Biochimica Et Biophysica Acta **688**(2): 381-387. doi: Doi 10.1016/0005-2736(82)90349-2. PMID: WOS:A1982NU46100011

Zborowski, J., and Demel, R.A. 1982b. Transfer properties of the bovine brain phospholipid transfer protein. Effect of charged phospholipids and of phosphatidylcholine fatty acid composition. Biochim Biophys Acta **688**(2): 381-387. PMID: 7104331

Zhang, W.X., Frahm, G., Morley, S., Manor, D., and Atkinson, J. 2009. Effect of bilayer phospholipid composition and curvature on ligand transfer by the alpha-tocopherol transfer protein. Lipids **44**(7): 631-641. doi: 10.1007/s11745-009-3310-x PMID: 19458973

Tables

Table 1: Equilibrium dissociation constants, $K_{d,}$ of PITPs to NBD-PC (n = 2; errors are difference about the mean)

Protein	K_d **(nM)**	**Maximum fluorescence counts**
PITPα	104 ± 13	347054
PITPβ	43 ± 8	89117
W203A/W204A (PITPα)	67 ± 12	159088
K61A (PITPα)	19 ± 4	130999
C95A (PITPα)	17 ± 2	13804
BSA	138 ± 19	39029

Table 2: Rate constants from NBD-PC reduction by sodium hydrosulfite. (n = 2; errors are difference about the mean)

Protein	**Rate Constant (s^{-1})**
PITPα	0.0099 ± 0.0001
PITPβ	0.0073 ± 0.0002
C95A (PITPα)	0.040 ± 0.0003

Figures

Figure 1: PC bound α-carbon traces of rat PITPα (Yoder et al. 2001, PDB:1T27, blue) and PITPβ (PDB: 2A1L, red) were aligned in PyMOL (Molecular Graphics System, v. 1.8 Schrödinger, LLC) through five iterative cycles resulting in a final RMSD of 0.346 Å over 221 amino acids. The bound PC in the PITPα is shown in black, and in PITPβ in grey. Numbering of the Trp residues is for PITPα.

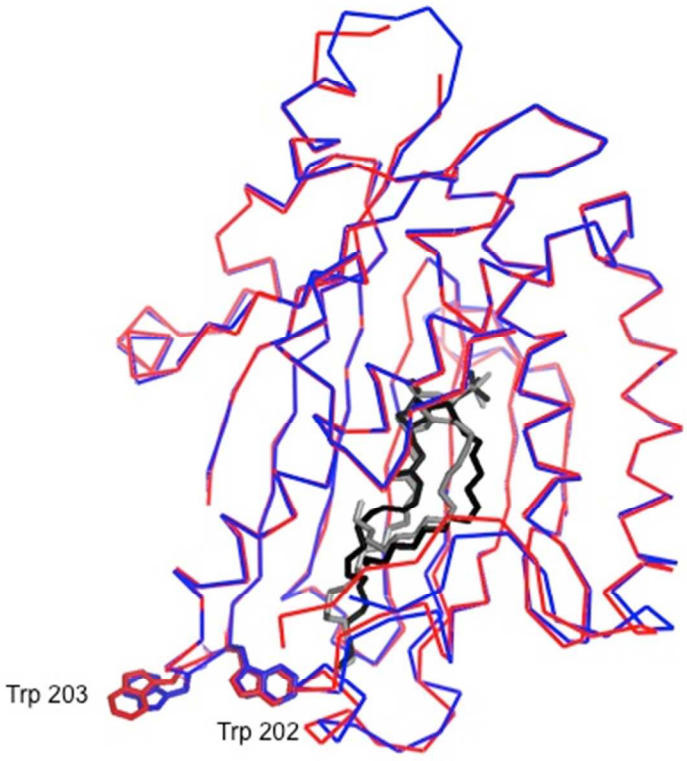

Figure 2: Orientation of A) Rat PITPα (PDB: 1T27) and B) PITPβ (PDB: 2A1L) as available from the OPM Database. Calculated boundaries between lipid head groups and acyl chain region are shown by small gray spheres.

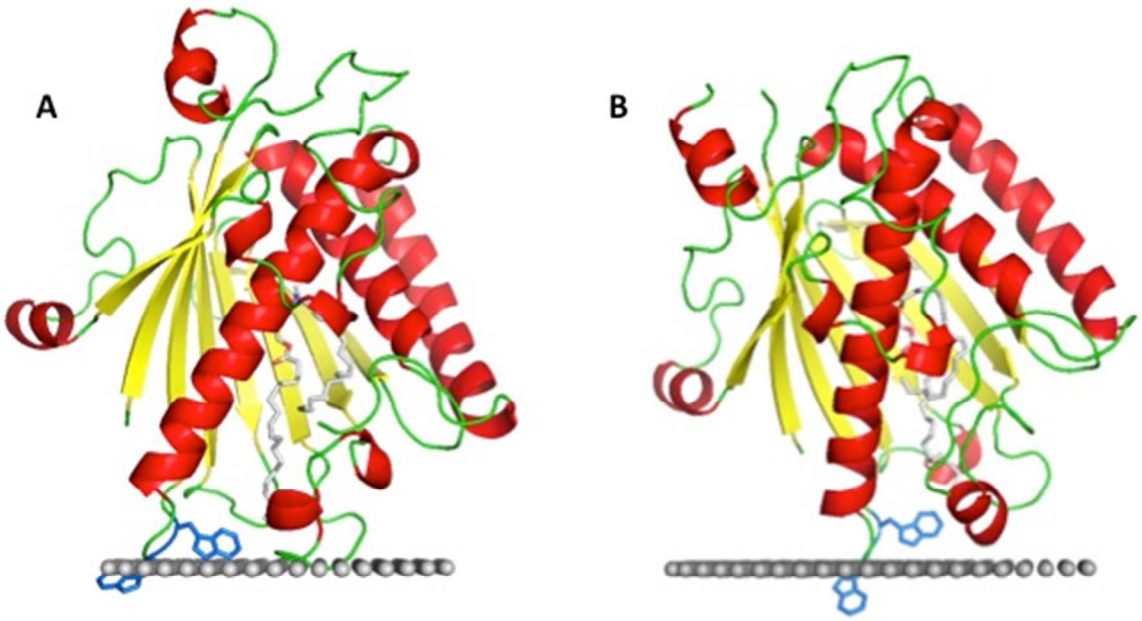

Figure 3: Plot of maximum specific mass of PITPα and PITPβ bound to DOPC lipid layers (n=2, errors are difference about the mean).

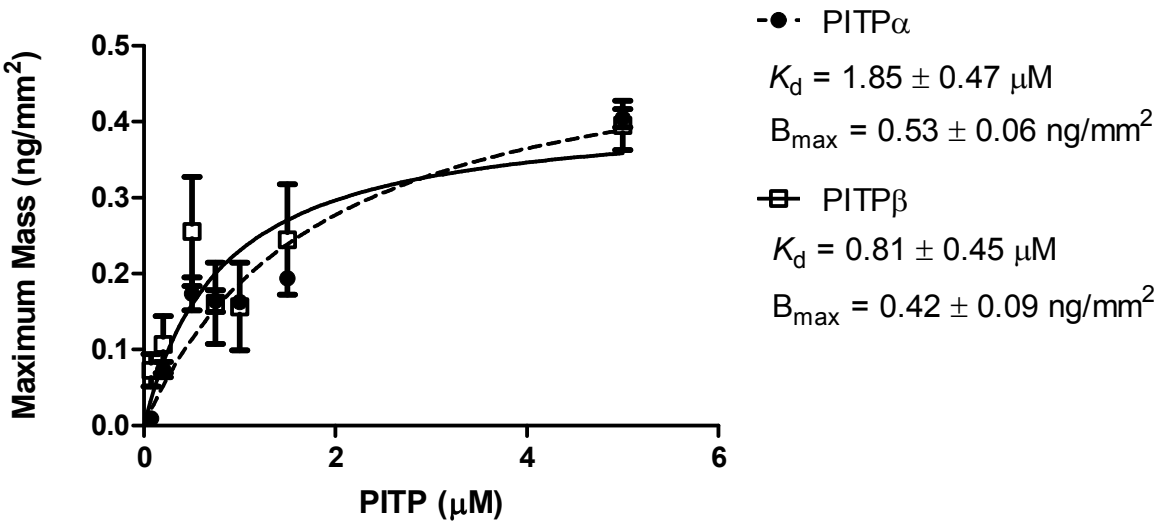

Figure 4: Comparison of maximum specific mass of PITPs (0.5 μM) adsorbed to immobilized DOPC lipid bilayers when the protein contains no ligand, bound PC, or bound PI (n=2-4). The asterisk (*) denotes that no detectable bound mass could be detected for PITPβ when pre-incubated with PI.

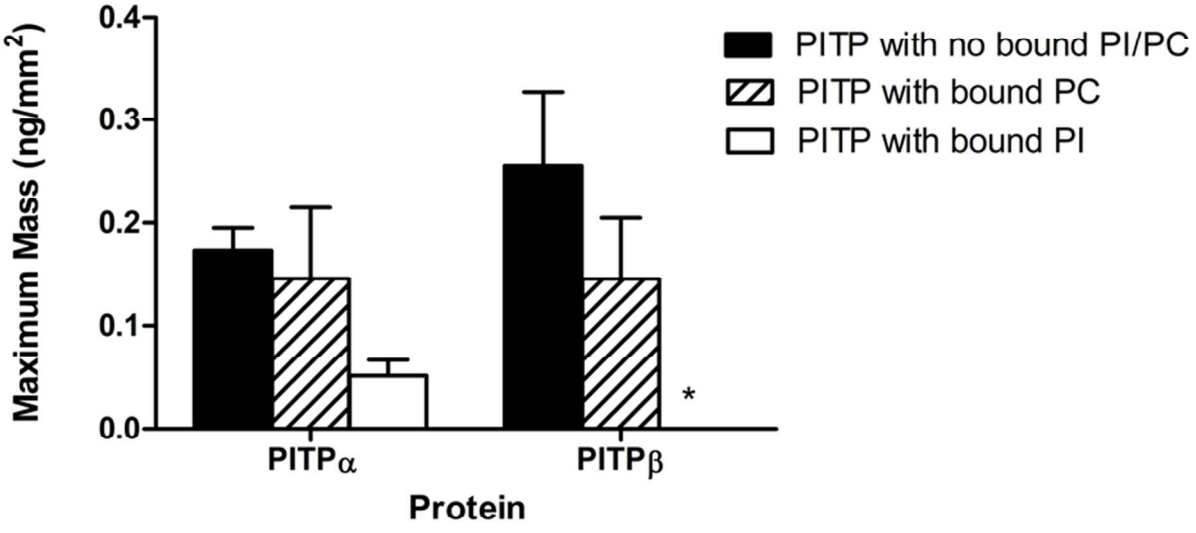

Figure 5: Unbound NBD-PC raw fluorescence trace in the absence and presence of lipid vesicles without FRET acceptor. Data are representative of a single measurement, however data were collected in triplicate.

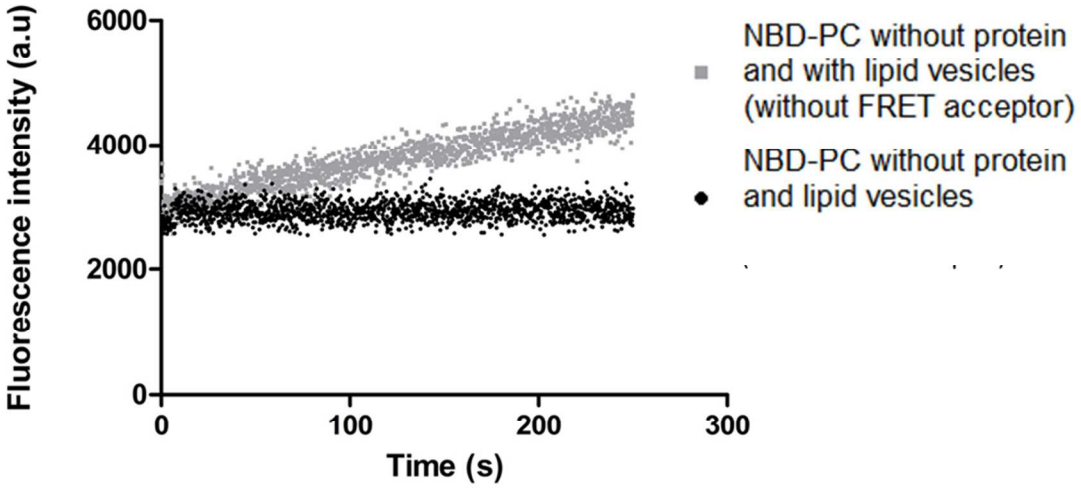

Figure 6: PITP-bound NBD-PC raw fluorescence trace in the absence and presence of lipid vesicles with FRET acceptor. Data shown are from one replicate, however measurements were performed in triplicates.

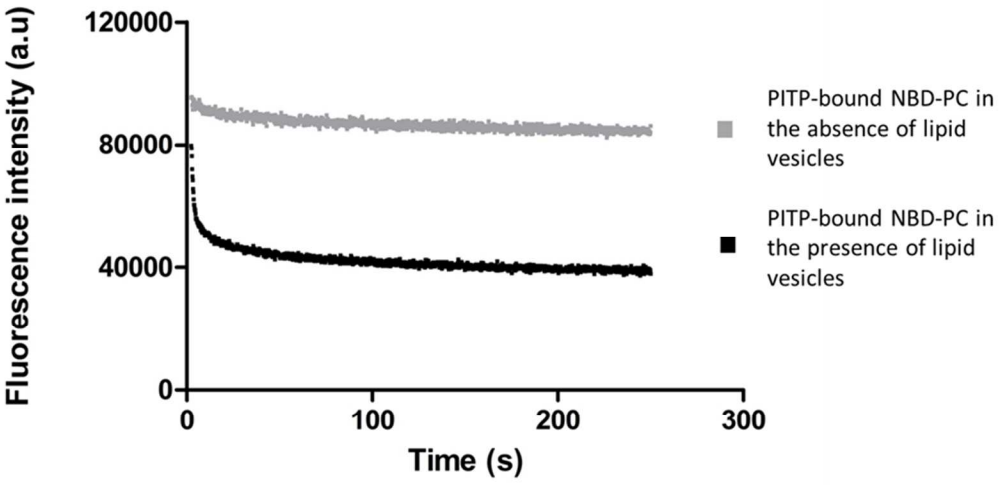

Figure 7: Comparison of NBD-PC transfer rates of wild-type PITPs and mutant PITPα (K61A) to PC SUVs and LUVs (n=3-6). Final lipid vesicle concentration after mixing was 100 μM

except for PITPβ measurements, which were 50 μM. Asterisks (*) denote unpaired t-test, p = 0.0001. The arrow denotes that transfer of NBD-PC could not be determined for the PITPα with LUVs.

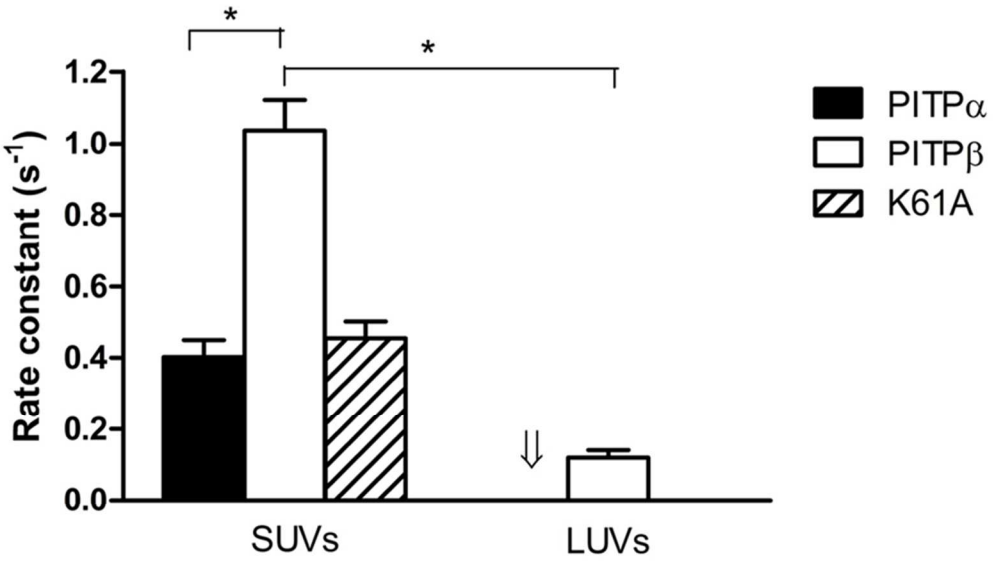

Figure 8: Raw data for the attempted transfer of NBD-PC by W203A/W204A and C95A (PITPα mutants) to SUVs. Negligible transfer of NBD-PC from protein to lipid vesicles were observed. Data are representative of one replicate, however measurements were done in triplicates.